EXACT DE RHAM SEQUENCES OF SPACES DEFINED ON MACRO-ELEMENTS IN TWO AND THREE SPATIAL DIMENSIONS

JOSEPH E. PASCIAK AND PANAYOT S. VASSILEVSKI

Abstract. This paper proposes new finite element spaces that can be constructed for agglomerates of standard elements that have certain regular structure. The main requirement is that the agglomerates share faces that have closed boundaries composed of 1-d edges. The spaces resulting from the agglomerated elements are subspaces of the original de Rham sequence of H^1-conforming, $H(\mathbf{curl})$ conforming, $H(\mathbf{div})$ conforming and piecewise constant spaces associated with an unstructured "fine" mesh. The procedure can be recursively applied so that a sequence of nested de Rham complexes can be constructed. As an illustration we generate coarser spaces from the sequence corresponding to the lowest order Nédélec spaces, lowest order Raviart–Thomas spaces, and for piecewise linear H^1-conforming spaces, all in three-dimensions. The resulting V-cycle multigrid methods used in preconditioned conjugate gradient iterations appear to perform similar to those of the geometrically refined case.

1. Introduction

The construction of coarse spaces from a finite element space on general unstructured mesh is an important task in several applications. For example, a suitable coarse space is needed in overlapping Schwarz methods to achieve convergence rates which are independent of the mesh size and the number of subdomains. A hierarchy of coarse spaces is also needed for the construction of multigrid (MG) algorithms for problems on both structured and unstructured meshes.

The exactness of the de Rham diagram (at the discrete level) plays an important role in the analysis of multigrid and overlapping Schwarz methods for the solution of the discrete systems resulting from approximating problems in $H(\mathbf{curl})$ and $H(\mathbf{div})$ (on structured meshes) [1, 2, 8, 9, 10]. Of course, the de Rham diagram identifies the kernel of the differential operator as the image of a differential operator applied to the preceding space and is thus fundamental. Often though, the analysis requires much more, e.g., the analysis of a multigrid algorithm in $H(\mathbf{curl})$ uses decompositions involving both H^1 and $H(\mathbf{div})$. The commutativity of the discrete de Rham diagram is also important in proving stability of certain mixed finite element methods (cf. [3, 6]). It is thus natural to ask whether one can get better behaved algebraic multigrid algorithms for these

Date: Beginning August 4, 2005; today is January 3, 2008.

1991 *Mathematics Subject Classification.* 78M10, 65F10, 65N30, 65N55.

Key words and phrases. mixed finite elements, exact sequences, algebraic multigrid, composite elements, agglomeration.

This work was performed under the auspices of the U.S. Department of Energy by Lawrence Livermore National Laboratory under Contract DE-AC52-07NA27344.

problems if the coarser spaces are designed so that the full discrete de Rham sequence is satisfied.

This paper offers a general construction of a hierarchy of discrete spaces based on element agglomeration satisfying the full de Rham sequence. Specifically, we start with the lowest order finite element spaces, H^1–conforming piecewise linears, lowest order Nédélec spaces, lowest order Raviart–Thomas spaces, and the space of (discontinuous) piecewise constants resulting from an unstructured triangulation of our domain. Coarser spaces are developed which are based on fairly general element, face, and edge agglomerations and lead to coarser H^1 vertex based spaces, $H(\mathbf{curl})$ (agglomerated) edge based spaces, $H(\mathbf{div})$ face based spaces and L^2 (agglomerated) element spaces. The resulting spaces satisfy the full de Rham diagram as do those with vanishing boundary components (zero mean value in the case of the L^2 space). Some constraints on the agglomerations are imposed so that they lead to objects with the expected topology, e.g., agglomerated edges, although no longer straight, form a connected path of fine grid edges, agglomerated faces, although no longer planar, do not contain holes (internal boundaries), etc.

Most of the work to date of a similar nature has been focused on constructing a hierarchy of pairs of spaces, where the first space of the pair is used to characterize the kernel of the differential operator in the second. For example, [4, 16, 15], set up pairs of spaces for the problem on $H(\mathbf{curl})$ where the first of the pair enables one to identify the discrete gradients in the second (on coarse meshes). The discrete gradients give the null–space of the discrete curl operator and is a fundamental part of the smoothing procedure used in the resulting algebraic multigrid algorithms [4, 16], [15].

Our main motivation to construct sequences of nested de Rham complexes that satisfy commutativity and exactness is in connection with the so–called element agglomeration algebraic multigrid (or AMGe for short). Element interpolation based AMG originated in [5] and its version utilizing element agglomeration was proposed in [12]. Further extensions are found in [7, 14, 18].

The hierarchy of finite element spaces proposed in the present paper allows for the construction of element agglomeration AMGe methods for the whole sequence of associated (H^1, $H(\mathrm{curl})$ and $H(\mathrm{div})$) bilinear forms which exhibit performance very similar to geometric MG on uniformly refined meshes. The ability to construct coarse counterparts of gradients, curls and divergence operators on general meshes has potential applications beyond AMGe for example in up–scaling of wide range of linear and non–linear PDEs. This potential application however is not the topic of the present paper.

We note that, as suggested by one of the referees, it may be possible to develop our results within the framework of differential forms (in a manner presented, e.g., in [11]). We choose not to use this approach.

The remainder of the present paper is structured as follows. In Section 2 we formulate the problem, introduce notation and state some facts to be used later on. The next section specifies the requirements on the topology of the agglomerated elements. The main construction of the coarse de Rham complexes in the two dimensional case is given in Section 4 while the three dimensional case is considered in Section 5. The application of the constructions to a simple composite element and some implementation details for a specific technique used to develop agglomerated element topology is given in Section

6. Finally, numerical illustration of the performance of the resulting AMGe methods is found in Section 6.2.

2. Preliminaries

Throughout this paper, we shall be concerned with discrete De Rham sequences on a domain D (or $\widetilde{D}$). The domain D will be either the original computational domain Ω or a mesh subdomain resulting from element agglomeration while $\widetilde{D}$ is an agglomeration of faces of a three dimensional mesh. The De Rham sequence at the continuous level is of the form

$$1(D) \longrightarrow H^1(D) \xrightarrow{\nabla} \boldsymbol{H}(curl;D) \xrightarrow{\nabla\times} \boldsymbol{H}(\mathrm{div};D) \xrightarrow{\nabla\cdot} L^2(D) \longrightarrow 0.$$

Here, $1(D)$ represents the one dimensional space of constants on D. This sequence is exact only if D is contractible, i.e., simply connected with a boundary which consists of one connected component. The sequence with homogeneous boundary conditions is of the form

$$0 \longrightarrow H^1_0(D) \xrightarrow{\nabla} \boldsymbol{H}_0(curl;D) \xrightarrow{\nabla\times} \boldsymbol{H}_0(\mathrm{div};D) \xrightarrow{\nabla\cdot} L^2(D)/1 \longrightarrow 0$$

and is also exact when D is contractible. For simplicity, we shall assume that D is simply connected with one boundary component.

We shall often need to know existence and uniqueness results for mixed systems on finite dimensional spaces. These results are standard and contained in those given in [6]. Let V and W be finite dimensional spaces, A be a symmetric quadratic form on V and B be a quadratic form on $V \times W$. We consider the mixed problem: Find $v \in V$ and $w \in W$ satisfying

$$\begin{aligned} A(v,\theta) + B(\theta,w) &= F(\theta) \quad \text{for all } \theta \in V, \\ B(v,q) &= G(q) \quad \text{for all } q \in W. \end{aligned} \tag{2.1}$$

Here F and G are functionals defined on V and W respectively.

Define

$$\mathrm{Ker}B = \{\theta \in V \ : \ B(\theta,q) = 0 \quad \text{for all } q \in W\}$$

and

$$\mathrm{Ker}B^t = \{q \in W \ : \ B(\theta,q) = 0 \quad \text{for all } \theta \in V\}.$$

We assume that $A(\theta,\theta) > 0$ for all nonzero θ in $\mathrm{Ker}B$. We then have the following proposition.

Proposition 2.1. *The mixed problem* (2.1) *has a solution $v \in V$ and $w \in W$ if and only if there is a $v_1 \in V$ satisfying $B(v_1,q) = G(q)$ for all $q \in W$. If there is a solution to* (2.1) *then v is unique and w is unique up to an element in $KerB^t$.*

We shall also use the following proposition concerning solutions with different test and trial spaces. It is a simple consequence of the Rank-Nullity theorem.

Proposition 2.2. *The problem: Find $v \in V$ satisfying*

$$B(v,q) = G(q) \quad \textit{for all } q \in W,$$

has a solution only if $G(q) = 0$ for all $q \in KerB^t$.

We comment that in what follows we will be using various bilinear forms defined in terms of L_2–inner products on surfaces or volumes. These shall be denoted $(\cdot,\ \cdot)$. We shall apply the above results on forms given by, for example, $a(\boldsymbol{u},\ \boldsymbol{v}) = (\boldsymbol{u},\ \boldsymbol{v})$ or $a(\boldsymbol{u},\ \boldsymbol{v}) = (\nabla\times\boldsymbol{u},\ \nabla\times\boldsymbol{v})$ and $b(\boldsymbol{u},\ w) = (\nabla\cdot\boldsymbol{u},\ w)$ or $b(\boldsymbol{u},\ \boldsymbol{v}) = (\nabla\times\boldsymbol{u},\ \boldsymbol{v})$, as well as two–dimensional counterparts (generally defined on surfaces).

3. Agglomeration: required properties

In this section, we discuss some of the assumptions which we shall make on our agglomeration procedure. Our goal is to keep the geometry of the agglomerated elements tractable.

We shall consider agglomeration in the two and three dimensional case. For simplicity, we shall start with initial (fine grid) partitioning into triangles or tetrahedrons, respectively. More general elements can be handled similarly.

Our goal is to generate a sequence of generalized meshes by applying a coarsening procedure. These meshes will be generated recursively. The structure of a generalized mesh of "size" h in two dimensions consists of sets of elements $\mathcal{T}_h$, edges E_h and vertices V_h. Elements are (open and) simply connected polygons (union of elements one fine level higher; on the finest level these are the original triangles). Edges are (open) connected one-dimensional manifolds made up of a connected path of fine grid edges, and vertices are single points. Elements and edges are always the interior of their closure and the union of the edges (and their endpoints) is connected. We make the following further assumptions:

(A.1) The elements, edges and vertices are disjoint.
(A.2) The union of the elements, edges, and vertices is all of $\bar{\Omega}$.
(A.3) The endpoints of an edge are vertices in V_h.
(A.4) The boundary of any element in $\mathcal{T}_h$ is the union of the edges in E_h and their endpoints.
(A.5) The intersection of an edge and the boundary of any element is either empty or all of the edge.

The three dimensional case is similar but a set of faces, F_h is included into the structure. Elements in 3D are polytopes (union of next level fine grid polytopes or on the finest level these are simply the original tetrahedrons). The elements are required to be contractible. Faces are open, simply connected two dimensional manifolds (union of faces of fine-grid elements). They are also the interior of their closure. The further assumptions are modified accordingly, i.e.,

(B.1) The elements, faces, edges and vertices are disjoint.
(B.2) The union of the elements, faces, edges, and vertices is all of $\bar{\Omega}$.
(B.3) The endpoints of an edge are vertices in V_h.
(B.4) The boundary of any face in F_h is union of edges in E_h and their endpoints.
(B.5) The boundary of any element in $\mathcal{T}_h$ is union of the closure faces in F_h. Also, the boundary of any element is simply connected surface.
(B.6) The intersection of an edge and the boundary of any face is either empty or all of the edge.

(B.7) The intersection of a face and the boundary of any element is either empty or all of the face.

Mesh structures satisfying the above conditions will be called consistent mesh structures.

Agglomeration involves building coarser mesh structures by putting together elements from a finer structure generated, for example, by a mesh partitioning algorithm. Algorithms that generate the topology of the agglomerated elements based on the topology of the fine–grid elements are well-developed (cf., for example, [12, 17]). They rely on operations on relation tables (boolean sparse matrices) that define the fine–grid connectivity. For example, they need relation table that lists the elements (as rows) and their faces (as columns), or relation table that lists faces (rows) and their edges (columns), and so on.

In practice, agglomeration algorithms relying on graph/mesh partitioners used to create (coarse) agglomerated structure from a consistent mesh structure are guaranteed to satisfy many of the consistent mesh assumptions. However, they may fail to automatically guarantee that:

(C.1) the elements of $\mathcal{T}_H$ are simply connected (and contractible in 3d),
(C.2) the edges are topologically paths of fine grid edges,
(C.3) the faces of F_H are simply connected,
(C.4) (A.1) or (B.1) to hold.

These conditions are, in general, not satisfied unless the partitioning of $\mathcal{T}_h$ is appropriately chosen. Most of the above irregularities can be remedied by post processing by refining agglomerates (note that these are union of fine–grid elements) at places where a desired property fails to hold. The most difficult part is to guarantee that the faces of the agglomerates are simply connected. In general, the development of such a partitioning for general meshes in the multilevel case is a formidable task.

4. The two dimensional case

In this section, Ω will be a simply connected polygonal domain in $\mathbb{R}^2$. We start with a triangulation of our domain $\Omega = \cup T$, $T \in \mathcal{T}_{h_0}$. Our development always starts with the lowest order finite elements associated with this mesh (without boundary conditions). Specifically, $\widetilde{S}_{h_0}(\Omega)$ is the set of continuous piecewise linears associated with the mesh, $\widetilde{R}_{h_0}(\Omega)$ is the lowest order Raviart-Thomas $\boldsymbol{H}(\text{div};\Omega)$-conforming finite element space and $\widetilde{M}_{h_0}(\Omega)$ consists of piecewise constants. Let D be a set domain formed from triangles in $\mathcal{T}_{h_0}$ i.e., D =interior$(\cup\tau)$ where τ runs over a subset of $\mathcal{T}_{h_0}$ and assume that D is simply connected. The above spaces satisfy the exact sequence

$$1(D) \longrightarrow \widetilde{S}_{h_0}(D) \xrightarrow{\nabla^\perp} \widetilde{R}_{h_0}(D) \xrightarrow{\nabla\cdot} \widetilde{M}_{h_0}(D) \longrightarrow 0. \tag{4.1}$$

Here $\nabla^\perp f = (-\frac{\partial f}{\partial y}, \frac{\partial f}{\partial x})$. Our goal is to develop subspaces of these based on element agglomeration which satisfy the analogous exact sequence for domains D made up of the larger elements.

We assume that we are given an element agglomeration procedure which produces a "coarser" consistent mesh $\mathcal{T}_H$, E_H, V_H from $\mathcal{T}_h$, E_h, and V_h as discussed in the previous section.

We will set up a recursive algorithm for developing sequences of the form of (4.1). We assume that we are given a sequence $\widetilde{S}_h(\Omega)$, $\widetilde{R}_h(\Omega)$, and $\widetilde{M}_h(\Omega)$ associated with $\mathcal{T}_h$. Initially, $h = h_0$ and $\mathcal{T}_h = \mathcal{T}_{h_0}$. We assume that the spaces associated with h satisfy

$$1(D) \longrightarrow \widetilde{S}_h(D) \xrightarrow{\nabla^\perp} \widetilde{R}_h(D) \xrightarrow{\nabla\cdot} \widetilde{M}_h(D) \longrightarrow 0. \tag{4.2}$$

Here $\widetilde{S}_h(D)$ denotes $\widetilde{S}_h(\Omega)$ restricted to D, etc. and D is any connected domain made up of elements of $\mathcal{T}_h$.

The spaces associated with h as well as those associated with H will have the following properties.

(D.1) The functions in $\widetilde{M}_h(\Omega)$ are always piecewise constant with respect to the elements $\mathcal{T}_h$.

(D.2) The degrees of freedom for $\widetilde{R}_h(\Omega)$ are associated with the edges. In fact, the basis function for $\widetilde{R}_h(\Omega)$ associated with $E \in E_h$ has a unit normal component along each $e \in E$ (e is an edge of the original triangulation $\mathcal{T}_{h_0}$) and has vanishing normal component on all $e \in E'$ with $E' \in E_h$ and $E' \neq E$. For the purpose of this definition, we must align the normals along the edge in a consistent manner, i.e., the normals should be all on the left or all on the right when traversing an edge.

(D.3) The degrees of freedom for $\widetilde{S}_h(\Omega)$ are associated with the nodes V_h. Functions in $\widetilde{S}_h(\Omega)$ are linear (with respect to edge length) along the edges in E_h.

When D is made up of elements of $\mathcal{T}_h$ and we define $S_h(D)$ and $R_h(D)$ to be the functions in $\widetilde{S}_h(D)$ and $\widetilde{R}_h(D)$ with vanishing boundary components. We also set $M_h(D)$ to be the functions in $\widetilde{M}_h(D)$ with zero mean value on D. We assume that

$$0 \longrightarrow S_h(D) \xrightarrow{\nabla^\perp} R_h(D) \xrightarrow{\nabla\cdot} M_h(D) \longrightarrow 0 \tag{4.3}$$

is exact. When D is a union of elements of $\mathcal{T}_H$, we define $S_H(D)$, $R_H(D)$ and $M_H(D)$ from $\widetilde{S}_H(D)$, $\widetilde{R}_H(D)$ and $\widetilde{M}_H(D)$ in an analogous way (once the latter have been defined).

Remark 4.1. The original mesh $\mathcal{T}_{h_0}$, E_{h_0} and V_{h_0} is consistent and the resulting spaces satisfy all of the assumptions which we made on the h spaces above.

Remark 4.2. It is also possible to use the techniques given below to develop exact sequences of the form

$$1(D) \longrightarrow \widetilde{S}_h(D) \xrightarrow{\nabla} \widetilde{K}_h(D) \xrightarrow{\nabla^\perp\cdot} \widetilde{M}_h(D) \longrightarrow 0$$

and

$$0 \longrightarrow S_h(D) \xrightarrow{\nabla} K_h(D) \xrightarrow{\nabla^\perp\cdot} M_h(D) \longrightarrow 0. \tag{4.4}$$

Here $\widetilde{K}_H(D)$ consists of edge elements in two spatial dimensions and coincides with the space obtained by rotating by $\pi/2$ the functions of $\widetilde{R}_H(D)$.

We now define the spaces associated with the H-mesh. Both $\widetilde{M}_H(\Omega)$ and $M_H(\Omega)$ were already defined.

We next define $\widetilde{R}_H(\Omega)$. The first requirement is that $\nabla\cdot\widetilde{R}_H(\Omega)$ is contained in $\widetilde{M}_H(\Omega)$, i.e., $\nabla\cdot r$ is piecewise constant on each element $T\in\mathcal{T}_H$ for any $r\in\widetilde{R}_H(\Omega)$. We consider the basis function associated with the edge $E\in E_H$. By definition, it has a normal component equal to 1 on each e in E and a vanishing normal component on each e in any other edge in E_H. This gives the normal components of the basis function r_E on the boundary of the elements so all we need to do is to define r_E inside the element. On each element $T\in\mathcal{T}_H$, we solve the mixed problem: Find $r_E\in\widetilde{R}_h(T)$ and $p\in M_h(T)$ satisfying

$$
\begin{aligned}
(r_E,\phi)_T+(\nabla\cdot\phi,p)_T&=0\quad\text{for all } \phi\in R_h(T),\\
(\nabla\cdot r_E,\theta)_T&=0\quad\text{for all } \theta\in M_h(T).
\end{aligned}
\tag{4.5}
$$

That the above problem is solvable can be seen as follows. The normal components of r_E are known on ∂T and we let $\tilde r_E$ be any function in $\widetilde{R}_h(T)$ having these normal components. We write $r_E=\tilde r_E+\psi$ with $\psi\in R_h(T)$. Then ψ satisfies the mixed system

$$
\begin{aligned}
(\psi,\phi)_T+(\nabla\cdot\phi,p)_T&=-(\tilde r_E,\phi)_T\quad\text{for all } \phi\in R_h(T),\\
(\nabla\cdot\psi,\theta)_T&=-(\nabla\cdot\tilde r_E,\theta)_T\quad\text{for all } \theta\in M_h(T).
\end{aligned}
\tag{4.6}
$$

It follows from the exactness of (4.3) (with $D=T$) at $M_h(T)$ and Proposition 2.1 that (4.6) has a unique solution. Moreover, it is easy to see that r_E is independent of the choice of extension $\tilde r_E$.

Now since any r_E is in $\widetilde{R}_h(T)$, $\nabla\cdot r_E$ is in $\widetilde{M}_h(T)$. Moreover, $\widetilde{M}_h(T)=M_h(T)\oplus 1(T)$ is an orthogonal decomposition. The second equation in (4.5) implies that $\nabla\cdot r_E$ is constant on T, i.e., $\nabla\cdot r_E$ is in $\widetilde{M}_H(T)$.

Using this definition on each element $T\in\mathcal{T}_H$ defines a basis function r_E on all of $\bar\Omega$. We define $\widetilde{R}_H(\Omega)$ to be the span of such functions. The above process shows that the basis functions can be assembled locally with respect to the elements $T\in\mathcal{T}_H$ and that $\nabla\cdot\widetilde{R}_H(\Omega)\subseteq\widetilde{M}_H(\Omega)$.

Remark 4.3. The term $(r_E,\phi)_T$ in (4.5) can be replaced by a lumped mass (diagonal) inner product to simplify the process of computing a basis in practice. This produces a different space $\widetilde{R}_H(\Omega)$ but one with similar properties.

We see that the functions in $\widetilde{R}_H(T)$ are completely determined by the values of the nodal components on the edges $E\in E_H$. We define $\pi_H^R:\widetilde{R}_h(T)\to\widetilde{R}_H(T)$ by

$$
\int_E(\pi_H^R r_h)\cdot n\,ds=\int_E r_h\cdot n\,ds,
$$

for each E in E_H, $E\subset\partial T$. The divergence theorem implies,

$$
\int_T\nabla\cdot(\pi_H^R r_h)\,da=\int_{\partial T}(\pi_H^R r_h)\cdot n\,ds=\int_{\partial T}r_h\cdot n\,ds=\int_T\nabla\cdot r_h\,da.
\tag{4.7}
$$

Let D be a domain made up of elements in $\mathcal{T}_H$ which is simply connected. The definition of π_H^R extends to an operator $\pi_H^R:\widetilde{R}_h(D)\to\widetilde{R}_H(D)$ and, because of (4.7), $\nabla\cdot\pi_H^R=$

$\pi_H^M \nabla\cdot$. Here π_H^M denotes the L^2 projection operator onto $\widetilde{M}_H(D)$. Now, by (4.2), if p is in $\widetilde{M}_H(D)$, then $p = \nabla \cdot \psi$ for some $\psi \in \widetilde{R}_h(D)$. The above commutativity implies that

$$p = \pi_H^M(\nabla \cdot \psi) = \nabla \cdot (\pi_H^R \psi), \tag{4.8}$$

i.e., $\nabla\cdot$ maps $\widetilde{R}_H(D)$ onto $\widetilde{M}_H(D)$ and the sequence (4.2) for $h = H$ is exact at $\widetilde{M}_H(D)$.

We next define $\widetilde{S}_H(\Omega)$ using a local construction which is designed so that $\nabla^\perp$ maps $\widetilde{S}_H(T)$ into $\widetilde{R}_H(T)$. Let v be a vertex of V_H. The basis function f_v corresponding to v is linear on each edge $E \in E_H$ so we need only define it in the interior of elements in $\mathcal{T}_H$. Note that since the normals are consistently aligned, the normal components of $\nabla^\perp f_v$ are constant on each edge E in E_H. The above construction produces a uniquely defined function $r_H \in \widetilde{R}_H(\Omega)$ satisfying $r_H \cdot n = (\nabla^\perp f_v) \cdot n$ on each edge $E \in E_H$. On each element $T \in \mathcal{T}_H$, $\nabla \cdot r_H$ is a constant. Moreover,

$$\int_T \nabla \cdot r_H \, da = \int_{\partial T} r_H \cdot n \, ds = \int_{\partial T} \frac{\partial f_v}{\partial \tau} \, ds = 0,$$

i.e., $\nabla\cdot r_H = 0$. Here we have oriented τ on each edge e of ∂T so that $(\nabla^\perp f_v)\cdot n = \partial f_v / \partial \tau$, i.e., τ is n rotated by $-\pi/2$. The exactness properties of (4.2) imply that there is a unique function $\tilde{f}_v \in \widetilde{S}_h(T)$ with $\nabla^\perp \tilde{f}_v = r_H$ and $\tilde{f}_v = f_v$ at one of the nodes of $\widetilde{S}_h(T)$. We set $f_v = \tilde{f}_v$ on T.

Actually, $f_v(x)$ for $x \in T$ can be recovered from the formula

$$f_v(x) = \int_\gamma r_H(s) \cdot n \, ds + f_v(x_0) \tag{4.9}$$

where x_0 is any point on ∂T, γ is a path from x_0 to x and n is the tangential direction τ along γ rotated by $\pi/2$. In practice, we need only recover the values of f_v on the vertices V_h. This is easily done by choosing a path which follows the edges of E_h on which $r_H \cdot n$ is constant.

This gives a basis for functions in $\widetilde{S}_H(\Omega)$. This construction guarantees that $\nabla^\perp$ maps $\widetilde{S}_H(D)$ into $\widetilde{R}_H(D)$. It is easy to see that $1(D)$ is a subspace of $\widetilde{S}_H(D)$. That $1(D)$ are the only functions in the kernel of $\nabla^\perp$ restricted to $\widetilde{S}_H(D)$ readily follows from the exactness of (4.2) at $\widetilde{S}_h(D)$.

The interpolation operator π_H^S is defined by nodal interpolation. It is straightforward to check that $\nabla^\perp \pi_H^S = \pi_H^R \nabla^\perp$ and hence the exactness of (4.2) for $h = H$ at $\widetilde{R}_H(D)$ follows immediately from the exactness at $\widetilde{R}_h(D)$ (as in (4.8)).

We have verified (4.2) for the sequence of subspaces $\widetilde{S}_H(D)$, $\widetilde{R}_H(D)$ and $\widetilde{M}_H(D)$. We next deal with the spaces with homogeneous boundary conditions.

It is clear from the way that nodal values were defined that $\nabla^\perp$ maps $S_H(D)$ into $R_H(D)$. That $\nabla\cdot$ maps $R_H(D)$ into $M_H(D)$ is a consequence of the divergence theorem and the fact that functions in $R_H(D)$ have vanishing normal component on ∂D. Finally, the interpolation operators π_H^S, π_H^R and π_H^M all map subspaces with boundary conditions into subspaces with boundary conditions and the commutativity properties still hold so the argument used in (4.8) and the exactness of (4.3) easily imply that (4.3) holds with the spaces $S_H(D)$, $R_H(D)$ and $M_H(D)$.

The technique for generating subspaces just developed is designed for developing nested multilevel spaces satisfying exact sequences of the form of (4.2) and (4.3). In general, these space lose the ability to reproduce constants and linears. The next proposition shows that local approximation properties are retained when the edges in E_H are straight lines.

Proposition 4.1. *Suppose that the edges in E_H are straight lines. Let $\widetilde{R}_2$ denote the two dimensional space of vector constants and $\widetilde{S}_3$ denote the three dimensional space of linear functions. Assume that D is a simply connected domain made up of elements in $\mathcal{T}_H$. If $\widetilde{R}_2 \subset \widetilde{R}_h(D)$ and $\widetilde{S}_3 \subset \widetilde{S}_h(D)$ then $\widetilde{R}_2 \subset \widetilde{R}_H(D)$ and $\widetilde{S}_3 \subset \widetilde{S}_H(D)$. Moreover, $\pi_H^R C = C$ for all $C \in \widetilde{R}_2$ and $\pi_H^S f = f$ for all $f \in \widetilde{S}_3$.*

Proof. Let C be in $\widetilde{R}_2$ and $T \in \mathcal{T}_H$ be an element of D. Then, since the edges of E_H are straight, $C \cdot n$ is constant along any edge E. This implies that $\pi_H^R C = r_C \in \widetilde{R}_H(D)$ has the same normal components as C on any subset of E_H. On $T \subset D$ with $T \in \mathcal{T}_H$, we write $r_C = C + \psi \equiv r_E + \psi$ where ψ satisfies (4.6). Note that the right hand side of the second equation in (4.6) is zero. Moreover, there exists a p in $M_h(T)$ satisfying

$$(p, \nabla \cdot \phi)_T = -(C, \phi)_T. \tag{4.10}$$

Indeed, we have

$$(C, \nabla^\perp \zeta)_T = 0 \quad \text{for all } \zeta \in S_h(T).$$

By the exactness of (4.3), $(C, \phi)_T = 0$ for all $\phi \in \mathrm{Ker}(\nabla \cdot)$ and the (unique) solvability of (4.10) follows from Proposition 2.2. It follows that $\psi = 0$ and p solving (4.10) is the solution of (4.6), i.e., $r_C = C$ on each element and hence all of D.

Now let f be in $\widetilde{S}_3$ and consider the interpolant of $f_v = \pi_H^S(f)$ in $\widetilde{S}_H(T)$. Then, since the edges of E_H are straight, $\nabla f_v \cdot \tau = (\nabla^\perp f_v) \cdot n = C \cdot n$ along any edge $E \in E_H$ (C not depending on E). By the first part of this proof, C is in $\widetilde{R}_H(T)$. Moreover f_v is given by (4.9) with $r_h = C$. Since $C = \nabla^\perp f$, f is also given by (4.9), i.e, f and f_v coincide. $\square$

5. The construction when Ω is in $\mathbb{R}^3$

In this section Ω is a contractible polyhedral domain contained in $\mathbb{R}^3$. We start with a mesh on our domain $\Omega = \cup T$, $T \in \mathcal{T}_{h_0}$. For convenience, we shall assume that the elements of the mesh are tetrahedrons. As in the two dimensional case, we start with the lowest order finite elements associated with this mesh. Specifically, $\widetilde{S}_{h_0}(\Omega)$ is the set of continuous piecewise linears associated with the mesh, $\widetilde{Q}_{h_0}(\Omega)$ is the lowest order curl-conforming Nédeléc (type one) elements, $\widetilde{R}_{h_0}(\Omega)$ is the lowest order Raviart-Thomas $\boldsymbol{H}(\mathrm{div};\Omega)$-conforming finite element space and $\widetilde{M}_{h_0}(\Omega)$ consists of piecewise constants. Let D be a domain formed from tetrahedra in $\mathcal{T}_{h_0}$. The above spaces satisfy the exact sequence

$$1(D) \longrightarrow \widetilde{S}_{h_0}(D) \xrightarrow{\nabla} \widetilde{Q}_{h_0}(D) \xrightarrow{\nabla\times} \widetilde{R}_{h_0}(D) \xrightarrow{\nabla\cdot} \widetilde{M}_{h_0}(D) \longrightarrow 0. \tag{5.1}$$

We again develop subspaces of these based on element agglomeration satisfying the analogous exact sequences.

We will set up a recursive algorithm for developing coarser subspaces satisfying sequences of the form of (5.1). We assume that we are given an element agglomeration procedure which produces a "coarser" consistent mesh $\mathcal{T}_H$, F_H, E_H, V_H from the given consistent mesh $\mathcal{T}_h$, F_h, E_h, and V_h as discussed in Section 2. Here h may be h_0 or the result of recursively applying the algorithm given below. We assume that we are given spaces $\widetilde{S}_h(\Omega)$, $\widetilde{Q}_h(\Omega)$, $\widetilde{R}_h(\Omega)$, and $\widetilde{M}_h(\Omega)$ associated with the mesh of size h satisfying (5.1) when D is a domain formed from elements in $\mathcal{T}_h$. As usual, $\widetilde{S}_h(D)$ denotes $\widetilde{S}_h(\Omega)$ restricted to D, etc.

As well as assuming (D.1) and (D.3) of the previous section, we further assume

(D.4) The degrees of freedom for $\widetilde{Q}_h(\Omega)$ are associated with the edges E_h. The basis function for $\widetilde{Q}_h(\Omega)$ associated with $E \in E_h$ has a unit tangential component along E (the tangential components are aligned so that they follow the edge when it is traversed in one direction).

(D.5) The degrees of freedom for $\widetilde{R}_h(\Omega)$ now correspond to the faces F_h. In this case, the basis function for $\widetilde{R}_h(\Omega)$ associated with $F \in F_h$ has a unit normal component on each $f \in F$ (f is a face of the original triangulation $\mathcal{T}_{h_0}$). Again the normals are aligned so that they either point outward or inward from either of the neighboring elements.

As in the two dimensional case, $M_h(D)$ is set to be the functions with zero mean value in D while the remaining spaces without the tildes are the subspace of functions with vanishing boundary components. We assume that

$$0 \longrightarrow S_h(D) \xrightarrow{\nabla} Q_h(D) \xrightarrow{\nabla\times} R_h(D) \xrightarrow{\nabla\cdot} M_h(D) \longrightarrow 0. \tag{5.2}$$

We shall also need to solve mixed problems on simply connected two dimensional manifolds $\widetilde{D}$ made up of faces $F \in F_h$. We define $\widetilde{K}_h(\widetilde{D})$ to be the restrictions of the tangential components of functions in $\widetilde{Q}_h(\Omega)$ to $\widetilde{D}$. We assume that such functions are determined by their tangential components along $E \in E_h$, $E \subset \widetilde{D}$. This is true for h_0 and will remain true in our subsequent constructions. Any such manifold $\widetilde{D}$ is made up of basic faces (triangles) τ from the h_0 mesh. On each such τ, functions in $\widetilde{K}_h(\widetilde{D})$ are polynomials of the form

$$k(x, y) = (a, b) + c(-y, x)$$

where x, y denotes a local orthogonal coordinate system on τ. The differential operator $\nabla^\perp \cdot f$ for vector functions in $\widetilde{K}_h(\widetilde{D})$ is then defined locally on τ by

$$\nabla^\perp \cdot f = (\frac{\partial f_2}{\partial x} - \frac{\partial f_1}{\partial y}).$$

Note that this operator is defined so that

$$(\nabla\times\phi) \cdot n = \nabla^\perp \cdot \phi_{tang}.$$

Here $\phi_{tang} = n \times \phi \times n$ denotes the tangential component of ϕ in the τ plane and n is either (unit) normal to τ. Functions of $\widetilde{R}_h(\Omega)$ have constant normal components on the faces in F_h, i.e., $\nabla^\perp \cdot k$ will be in $\widetilde{M}_h(\widetilde{D})$ for $k \in \widetilde{K}_h(\widetilde{D})$. Here $\widetilde{M}_h(\widetilde{D})$ is defined to be piecewise constant functions on $\widetilde{D}$ with respect to the partition $F \in F_h$, $F \subset \widetilde{D}$. We will assume that, by construction, the following sequence is exact:

$$K_h(\widetilde{D}) \xrightarrow{\nabla^\perp\cdot} M_h(\widetilde{D}) \longrightarrow 0. \tag{5.3}$$

Here $K_h(\widetilde{D})$ denotes those functions in $\widetilde{K}_h(\widetilde{D})$ with vanishing tangential components on $\partial\widetilde{D}$ and $M_h(\widetilde{D})$ is the set of functions in $\widetilde{M}_h(\widetilde{D})$ with zero mean value on $\widetilde{D}$.

Remark 5.1. The validation of (5.3) in the case of h_0 is not trivial. Its complete analysis depends on regularity for elliptic problems on the manifold $\widetilde{D}$. Such regularity estimates seem likely but, as far as we know, cannot be quoted for some of the nonplanar domains $\widetilde{D}$ resulting from agglomeration.

We now define the spaces associated with the H-mesh. Both $\widetilde{M}_H(\Omega)$ and $M_H(\Omega)$ were already defined.

The construction of $\widetilde{R}_H(\Omega)$ is similar to the two dimensional constructions. The basis function associated with the face $F \in F_H$ is set element by element. On the element T it is defined by first setting its boundary normal components (one on the triangles of the face F and zero on the triangles of the remaining faces of ∂T) and subsequently defining it in the interior by solving the mixed problem (4.5). This is completely analogous to the case of two spatial dimensions and so no further details will be given. Commuting projections are defined similarly with integrals over edges replaced by integrals over faces. This leads to exactness at $\widetilde{M}_H(D)$ in (5.1) with $h = H$ and D a domain made up of elements in $\mathcal{T}_H$.

The construction of the space $\widetilde{Q}_H(D)$ is a little more interesting as it will require mixed problems both on the faces and the elements. Let E be in E_H, $E \subset \bar{D}$. We construct the basis function q_E corresponding to E on an element $T \in \mathcal{T}_H$, $T \subset D$. To do this, we first need to construct its boundary components on ∂T and subsequently define it in the interior of T. Let F be a face in F_H, $F \subset \partial T$. For $\nabla\times q_E$ to be in $\widetilde{R}_H(T)$, it must have a constant normal component on each face F in F_H. We impose this condition by setting up a mixed problem on face in F_H. To do this, we fix $F \in F_H$. The tangential component of q_E along F is in $\widetilde{K}_h(F)$. Now the tangential components of q_E along E are all set to one while its tangential components along all other edges of $E \in E_H$, $E \subset \partial F$ are set to zero. This defines the tangential components of q_E on the edges of ∂F. The tangential components of q_E on F (denoted by $q_E(tang)$) is determined on the interior of F by the solution of the mixed problem: Find $q_E(tang) \in \widetilde{K}_h(F)$ with boundary values as discussed above and $p \in M_h(F)$ satisfying

$$\begin{aligned} (q_E(tang), \phi)_F + (\nabla^\perp\cdot\phi, p)_F &= 0 \quad \text{for all } \phi \in K_h(F), \\ (\nabla^\perp\cdot q_E(tang), \theta)_F &= 0 \quad \text{for all } \theta \in M_h(F). \end{aligned} \tag{5.4}$$

As usual, we write $q_E(tang) = \tilde{q}_E + \psi$ where $\tilde{q}_E$ has the required tangential components on ∂F and $\psi \in K_h(F)$ solves

$$\begin{aligned} (\psi, \phi)_F + (\nabla^\perp\cdot\phi, p)_F &= -(\tilde{q}_E, \phi)_F \quad \text{for all } \phi \in K_h(F), \\ (\nabla^\perp\cdot\psi, \theta)_F &= -(\nabla^\perp\cdot\tilde{q}_E, \theta) \quad \text{for all } \theta \in M_h(F). \end{aligned} \tag{5.5}$$

The unique solvability of this problem follows from (5.3) with $\widetilde{D} = F$ and Proposition 2.1. This defines a tangential vector field on F which we use to provide the tangential components of q_E on F. The second equation of (5.4) implies that

$$\nabla^{\perp} \cdot q_E(tang) = (\nabla \times q_E) \cdot n = C_F \text{ on } F. \tag{5.6}$$

Here q_E is any function with tangential components on F given by $q_E(tang)$ and C_F is a constant.

We repeat the above construction on each face to define the tangential components of q_E on each face F of ∂T. These tangential fields satisfy (5.6) and therefore there is a unique function in $r_H \in \widetilde{R}_H(T)$ with $r_H \cdot n = C_F$ on each face $F \in F_H$, $F \subset T$. The value for q_E on T is computed by solving the mixed problem: Find $q_E \in \widetilde{Q}_h(T)$ (with boundary components as discussed above) and $r \in R_h(T)$ satisfying

$$\begin{aligned} (q_E, \phi)_T + (\nabla \times \phi, r)_T = 0 \quad &\text{for all } \phi \in Q_h(T), \\ (\nabla \times q_E, \theta)_T = (r_H, \theta)_T \quad &\text{for all } \theta \in R_h(T). \end{aligned} \tag{5.7}$$

As usual, we set $q_E = \tilde{q}_E + \psi$ where $\tilde{q}_E$ is any function in $\widetilde{Q}_h(T)$ with the above tangential components on ∂T and $\psi \in Q_h(T)$ solves

$$\begin{aligned} (\psi, \phi)_T + (\nabla \times \phi, r)_T = -(\tilde{q}_E, \phi)_T \quad &\text{for all } \phi \in Q_h(T), \\ (\nabla \times \psi, \theta)_T = (r_H, \theta)_T - (\nabla \times \tilde{q}_E, \theta)_T \quad &\text{for all } \theta \in R_h(T). \end{aligned} \tag{5.8}$$

The solvability of (5.8) follows from Proposition 2.1 once we show that there is at least one solution $\psi_1 \in Q_h(T)$ to the second equation in (5.8). In this case, r is not unique.

We exhibit ψ_1 as follows. By the construction of r_H, $\nabla \cdot r_H$ is constant on T. Moreover,

$$\begin{aligned} (\nabla \cdot r_H, 1)_T = (r_H \cdot n, 1)_{\partial T} &= \sum_{F \in \partial T} (\nabla^{\perp} q_H(tang), 1)_F \\ &= \sum_{F \in \partial T} (q_H(tang) \cdot \tau, 1)_{\partial F} = 0. \end{aligned}$$

This implies that $\nabla \cdot r_H = 0$, i.e., $r_H = \nabla \times q_h$ for some $q_h \in \widetilde{Q}_h(T)$. Now $r_H \cdot n = (\nabla \times \tilde{q}_E) \cdot n$ so $\nabla \times (q_h - \tilde{q}_E)$ is in $R_h(T)$. As its divergence clearly vanishes, (5.2) implies that there is a $\psi_1 \in Q_h(T)$ satisfying $\nabla \times \psi_1 = \nabla \times (q_h - \tilde{q}_E)$. This defines q_E on each $T \in \mathcal{T}_H$ and hence all of $\bar{D}$ (indeed, all of $\bar{\Omega}$).

We next verify that (5.3) holds for $h = H$. Let $\widetilde{D}$ denote any connected domain made from faces in F_H. It easily follows from (5.4) that $\nabla^{\perp} \cdot$ maps $\widetilde{K}_H(\widetilde{D})$ into $\widetilde{M}_H(\widetilde{D})$. This and integration by parts implies that $\nabla^{\perp} \cdot$ maps $K_H(\widetilde{D})$ into $M_H(\widetilde{D})$. The projector $\pi_H^K : \widetilde{K}_h(\widetilde{D}) \to \widetilde{K}_H(\widetilde{D})$ is based on integration of the tangential components along edges in $E \in E_H$, $E \subset \widetilde{D}$ while the projector associated with $\pi_H^{\tilde{M}} : \widetilde{M}_h(\widetilde{D}) \to \widetilde{M}_H(\widetilde{D})$ is the $L^2(\widetilde{D})$-projector. That (5.3) is exact at $M_H(\widetilde{D})$ follows from the commutativity identity $\pi_H^{\tilde{M}} \nabla^{\perp} \cdot \phi = \nabla^{\perp} \cdot \pi_H^K \phi$ for all $phi \in \widetilde{K}_h(\widetilde{D})$.

The projector π_H^Q associated with $\widetilde{Q}_H(\Omega)$ is also defined by integrals of the tangential components along edges $E \in E_H$. It is easily seen from the above construction that

$$\nabla \times (\pi_H^Q q) = \pi_H^R (\nabla \times q) \quad \text{for all } q \in \widetilde{Q}_h(D),$$

for any D made up of elements of $\mathcal{T}_H$. Indeed, for $q \in \widetilde{Q}_h(T)$ with F being any face $F \in F_H$, $F \subset \partial T$,

$$\begin{aligned}\int_F (\nabla\times(\pi_H^Q q)) \cdot n \, da &= \int_F \nabla^\perp(\pi_H^Q q)(tang) \, da = \int_{\partial F} (\pi_H^Q q) \cdot \tau \, ds \\ &= \int_{\partial F} q \cdot \tau \, ds = \int_F (\nabla\times q) \cdot n \, da = \int_F (\pi_H^R(\nabla\times q)) \cdot n \, da.\end{aligned}$$

The exactness of (5.1) for $h = H$ at $\widetilde{R}_H(D)$ immediately follows from the exactness of (5.1) (with h).

Remark 5.2. The computation of q_E on T given by (5.7) can be replaced by the alternative mixed problem: Find $q_E \in \widetilde{Q}_h(T)$ with the same boundary components and $p \in S_h(T)$ satisfying

$$\begin{aligned}(\nabla\times q_E, \nabla\times\phi)_T + (\nabla p, \phi)_T &= (r_H, \nabla\times\phi)_T \quad \text{for all } \phi \in Q_h(T), \\ (q_E, \nabla\theta)_T &= 0 \quad \text{for all } \theta \in S_h(T).\end{aligned} \tag{5.9}$$

The above equation has a unique solution q_E which coincides with that of (5.7) (and $p = 0$). The system (5.9) may be more convenient to solve in practice when building the basis functions.

We define $\widetilde{S}_H(\Omega)$ using a local construction which is designed so that ∇ maps $\widetilde{S}_H(T)$ into $\widetilde{Q}_H(T)$ for each $T \in \mathcal{T}_H$. Let v be a vertex of in V_H. The basis function f_v corresponding to v is linear on each edge $E \in E_H$. This determines f_v and the tangential component $\nabla f_v \cdot \tau$ on every edge $E \in E_H$. Let q_E be the unique function in $\widetilde{Q}_H(T)$ with the above tangential components. Let $F \in F_H$ be a face of T. Then $(\nabla\times q_E) \cdot n$ is constant on F and

$$((\nabla\times q_E) \cdot n, 1)_F = (\nabla^\perp q_E(tang), 1)_F = (\nabla f_v \cdot \tau, 1)_{\partial F} = 0,$$

i.e., $(\nabla\times q_E) \cdot n$ is zero on F. This implies that $\nabla\times q_E = r_E$ has vanishing normal components on each face $F \in F_H$ of ∂T, i.e., $r_E = \nabla\times q_E$ vanishes identically on T. By the exactness of (5.1), there is a unique (up to a constant) function $f_v \in \widetilde{S}_h(T)$ with $\nabla f_v = q_E$. As in the two dimensional case, the function can be recovered from the formula

$$f_v(x) = \int_\gamma q_E(s) \cdot \tau \, ds + f_v(x_0) \tag{5.10}$$

where x_0 is any point on ∂F, γ is a path from x_0 to x and τ is the tangential direction along γ. In practice, we need only recover the values of f_v on the vertices V_h. This is easily done by choosing a path which follows the edges of E_h on which $q_E \cdot \tau$ is constant.

The projector π_H^S is defined by nodal interpolation. A consequence of the above construction is that this projector satisfies a commuting diagram with ∇ and π_H^Q. The exactness of (5.1) with $h = H$ at $\widetilde{Q}_H(D)$ follows easily. The exactness at $\widetilde{S}_H(D)$ follows as in the two dimensional case. Finally, the exactness of the sequence (5.2) with spaces satisfying homogeneous boundary conditions also follows as in the two dimensional case.

The three dimensional construction will preserve approximation provided that the faces are planar and the edges are straight.

Proposition 5.1. *Suppose that the faces in F_H are planar and the edges in E_H are straight lines. Let $\widetilde{R}_3$ denote the three dimensional space of vector constants and $\widetilde{S}_4$ denote the four dimensional space of linear functions. Assume that D is contractible domain made up of elements in $\mathcal{T}_H$. If $\widetilde{R}_3 \subset \widetilde{R}_h(D)$, $\widetilde{R}_3 \subset \widetilde{Q}_h(D)$, and $\widetilde{S}_4 \subset \widetilde{S}_h(D)$ then $\widetilde{R}_3 \subset \widetilde{R}_H(D)$, $\widetilde{R}_3 \subset \widetilde{Q}_H(D)$, and $\widetilde{S}_4 \subset \widetilde{S}_H(D)$. Moreover, $\pi_H^R C = C$, $\pi_H^Q C = C$ and $\pi_H^S f = f$ for all $C \in \widetilde{R}_3$ and $f \in \widetilde{S}_4$.*

Proof. The case of $\widetilde{R}_3 \subset \widetilde{R}_H(D)$ and π_H^R is completely analogous to the two dimensional case.

Let C be in $\widetilde{R}_3$. As the edges of E_H are straight, $C \cdot \tau$ is constant on each edge $E \in E_H$ and $q_C = \pi_H^Q(C) \in \widetilde{Q}_H(D)$ takes on these values. We need to show that $q_C = C$. Let F be a face. We need to first show that the function $q_E(tang)$ constructed above satisfying these boundary values is the tangential component $C(tang)$ of C on F. The argument is similar to that used in Proposition 4.1. We take $\tilde{q}_E = C$ on F and subsequently show that $\psi = 0$ solves (5.5). By Proposition 2.2, it suffices to show that $(C(tang), \phi)_F = 0$ for any $\phi \in K_h(F)$ satisfying $\nabla^\perp \cdot \phi = 0$. As ϕ has vanishing tangential components, $\phi = \nabla\theta$ for $\theta \in H_0^1(F)$ and so

$$(C(tang), \phi)_F = \int_{\partial F} C(tang) \cdot n_F \; \theta \; ds = 0.$$

Similarly, to show that $q_C = C$ in the element T we need to show that $(C, \phi)_T = 0$ for any $\phi \in Q_h(T)$ satisfying $\nabla \times \phi = 0$. It follows that $\phi = \nabla\theta$ with $\theta \in H_0^1(T)$ and so $(C, \phi)_T = 0$ by integration by parts. This shows that $\widetilde{R}_3 \subset \widetilde{Q}_H(D)$ and $\pi_H^Q C = C$.

The argument showing that $\widetilde{S}_4 \subset \widetilde{S}_H(D)$ and $\pi_H^S f = f$ is completely analogous to that used in the two dimensional case. $\square$

6. Agglomerated elements

In this section, we provide some examples illustrating the application of the constructions in the previous sections.

A simple composite element. We start with $h = h_0$ so that the spaces appearing in (4.2) and (4.3) come from the standard lowest order elements and the triangulation results from an original partitioning of Ω into quadrilaterals which are subsequently subdivided into triangles alone a diagonal. The elements of $\mathcal{T}_h$ are the resulting triangles while those of $\mathcal{T}_H$ are the original quadrilaterals. The techniques of Section 4 give rise to composite Raviart-Thomas like spaces on quadrilaterals. This example can be generalized in many directions, for example, it can also be used to develop sequences of function spaces based on meshes with hanging nodes.

From the construction of the previous section, we note that we have not eliminated any nodes by agglomeration. This means that $S_H(\Omega) = S_h(\Omega)$.

The agglomeration does lead to a Raviart-Thomas space based on composite elements. Let the nodes and edge dofs of a composite element be denoted as in Figure 1. For convenience, we scaled the edge degrees of freedom (a, b, c, d and α below) so that their value represents the value of the normal of the function times the length of the edge. We orient the normals so that they point outward of the quadrilateral while the normal on the diagonal points from τ_1 to τ_2. The value of α is a slave to the remaining edge values.

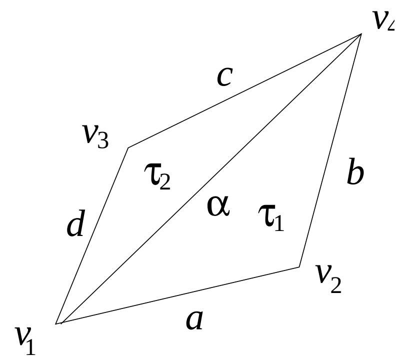

FIGURE 1. A composite quadrilateral element.

A simple computation shows that

$$\alpha = \frac{A_2(-a-b) + A_1(c+d)}{(A_1 + A_2)}.$$

Here A_1 and A_2 denote the area of the triangles τ_1 and τ_2, respectively. The local element matrices associated with this quadrilateral can then be assembled in a straightforward manner.

Proposition 4.1 and a Bramble-Hilbert argument shows that the subspaces $\widetilde{R}_H(\Omega)$ and $R_H(\Omega)$ retain the convergence properties of the original spaces $\widetilde{R}_h(\Omega)$ and $R_h(\Omega)$.

6.1. **Topology of agglomerated elements.** Element agglomeration MG was studied in [12, 17] where algorithms to construct agglomerated elements (AEelem), faces (AEface) and edges (AEedge) were formulated. Our purpose here is not to go into an in-depth review of the algorithms but rather give the reader some indications of the possible issues and their solutions.

The basic idea of an agglomeration starts with partitioning of the elements, each partition represents an AEelem on the coarser level. This can be obtained by applying a mesh partitioning procedure such as **metis** (e.g., [13]) . Further partitioning of the resulting agglomerated elements can be carried out to ensure, for example, simply connected elements in two dimensions or contractible elements in three. Next, AEfaces are defined by gathering together fine grid faces with common neighboring AEelems (of course, faces which are interior to elements are discarded). This AEface list can be further partitioned to attempt to satisfy the properties listed in Section 3. The initial AEedge list is defined by gathering together fine grid edges with common neighboring AEfaces. Again, this list may be further partitioned to attempt to achieve the properties of Section 3. Finally, the coarse vertices are defined to be the endpoints of the AEedges. We refer to the initial AEface and AEedge lists as minimal. The maximal structure would be to further partition these lists using all possible fine grid faces and edges. Of course, the maximal structure defeats the purpose as we seek agglomerated structures with significantly fewer elements, faces, edges and vertices.

Even the above strategy may not be general enough. In our implementation, for example, to obtain the desired properties for the AEedges, we sometimes had to locally refine the AEelems.

We illustrate some of the issues which arise with two examples. A given domain (a cube and a composite polytope, shown in Figs. 3 and 5, respectively) is first triangulated by a relatively coarse unstructured mesh. Then, the actual mesh is obtained by several levels of uniform refinement. The first such levels the agglomerates are simply the refined coarse elements. After that, the next level agglomerates are obtained by the mesh partitioner **metis**.

The application of the mesh partitioner **metis** led to some non–standard (but often occurring) situations. Even in two dimensions, when using the minimal AEface-AEedge structure, it is possible to have an endpoint of an AEedge coinciding with an interior point of another AEedge. This is illustrated in Figure 2 where E_i, $i = 1, \dots, 4$ denote agglomerated elements. In this case, (a,b) is an AEedge with an interior point c being a coarse vertex. This violates (A.1). This type of trouble appears also in three spatial dimensions and can lead to additionally a coarse vertex or AEedge ending up in the interior of an AEface or an AEedge without endpoints.

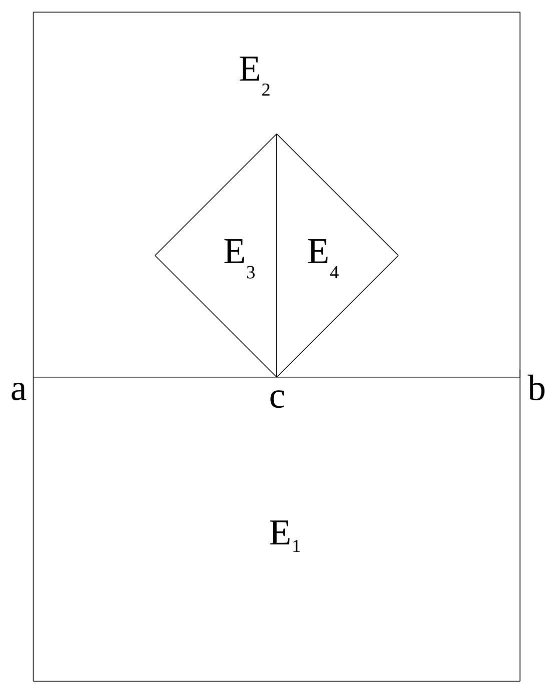

FIGURE 2. Agglomeration trouble in two dimensions.

6.2. **Multigrid based on agglomerated elements.** The technique developed in the present paper can be applied recursively to develop three sequence of spaces based on recursive element agglomeration. Each set of spaces satisfy exact sequences of the form (4.2) and (4.3) and also satisfy commuting diagrams between levels. This sequence can be used to develop new algebraic multigrid algorithms.

We consider the parameter dependent $\boldsymbol{H}_0(\mathbf{curl})$ and $\boldsymbol{H}_0(\mathrm{div})$ bilinear forms

$$(\nabla\times\boldsymbol{u},\ \nabla\times\boldsymbol{v}) + \delta\ (\boldsymbol{u},\ \boldsymbol{v}), \quad (\nabla\cdot\boldsymbol{u},\ \nabla\cdot\boldsymbol{v}) + \delta\ (\boldsymbol{u},\ \boldsymbol{v}),$$

for $\delta = 1$ and $\delta = 10^{-3}$. The respective stiffness matrix A_0 corresponds to the lowest order Nédélec or Raviart–Thomas space associated with the given domain with homogeneous Dirichlet boundary conditions $\boldsymbol{u} \times n = 0$ or $\boldsymbol{u} \cdot n = 0$ imposed. The coarse level spaces are associated with the recursively constructed agglomerated elements as explained in the preceding section. In the tables below we compared the number of iterations of two preconditioned conjugate gradient methods; one is the PCG (preconditioned conjugate gradient) with symmetric Gauss–Seidel preconditioner (denoted by GS) and the second one is the PCG with a V(1,1)–cycle MG. The MG V–cycle exploits the interpolation operators constructed by the procedure from the preceding section, standard forward (from fine–to–coarse levels) Gauss–Seidel smoothing as well as forward (from fine–to–coarse levels) Gauss–Seidel smoothing based on the gradients of the nodal (Lagrangian) basis functions viewed as elements of the Nédélec spaces (i.e., the respective Hiptmair smoother). From coarse–to–fine levels we use backward smoothing (both standard and Hiptmair ones). This symmetrizes the V(1,1)–cycle (the symmetry is needed in the PCG method). Both PCG methods are stopped after the preconditioned residual is reduced by a factor of 10^6. The smoothing in the downward part of the V–cycle for the $\boldsymbol{H}(\mathrm{div})$ problem is constructed similarly; namely, a forward face–dof based GS is followed by a edge–based forward GS (i.e., the $\boldsymbol{H}(\mathrm{div})$ counterpart of Hiptmair smoother) utilizing the fact that the $\nabla\times\boldsymbol{\theta}$ for every edge–based agglomerated Nédélec basis function $\boldsymbol{\theta}$ belongs to the respective agglomerated Raviart–Thomas space. In the upward (coarse–to–fine) direction the V–cycle is symmetrized by performing the smoothing in reverse order (and forward GS replaced by backward GS).

We also show the performance in a preconditioned CG method the V–cycle (GS–based) applied to the Laplace equation on the same mesh and using the agglomerated vertex–based spaces.

In the tables, we also report, the size of the fine–grid problem (number of elements and number of degrees of freedom (edges, faces or vertices) as well as two measures of MG efficiency "arithmetic" and "operator" complexities, (denoted "arithm." and "oper." respectively). These two measures are commonly used in the AMG (algebraic MG) literature. The "arithm." is defined as the ratio number of fine grid dofs over the sum over the levels of all number of dofs, whereas the "oper." is defined as the number of non–zeros of the fine–grid stiffness matrix divided by the sum over the levels of the number of non-zeros of all stiffness matrices. Finally, the fairly minor dependence on the parameter δ on the convergence of the MG method in the case of $\boldsymbol{H}(\mathrm{curl})$ problems is illustrated in Tables 6.5 - 6.6. The situation is similar for $\boldsymbol{H}(\mathrm{div})$ as well.

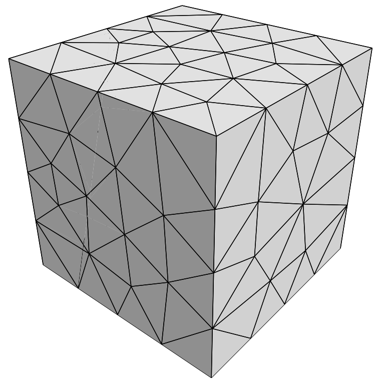

FIGURE 3. Initial mesh on the unit cube.

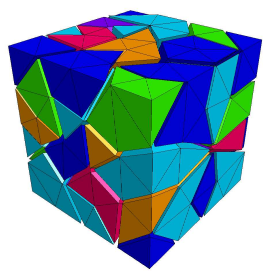

FIGURE 4. Partitioned cube.

ℓ	$\boldsymbol{H}$(curl)			$\boldsymbol{H}$(div)			Laplace		
	N	MG	GS	N	MG	GS	N	MG	GS
5	293224	11	> 1999	492032	17	> 1999	43881	9	46
4	37940	10	973	62336	15	> 1999	5941	7	22
3	5074	8	306	8000	12	750	867	6	10
2	722	6	89	1052	9	230	145	4	4

TABLE 6.1. Number of iterations for problems on the unit cube with unstructured mesh; $\delta = 10^{-3}$.

We comment at the end that the setup cost of constructing the hierarchy of coarse problems is of the same order as for any element agglomeration AMGe method. At a given level k, the cost is $\mathcal{O}(N_k)$ for a problem of size N_k. The constant in the $\mathcal{O}$-term can be fairly large. In the present setting, it reflects the fact that we solve local saddle–point

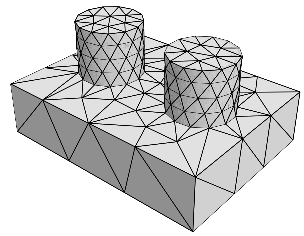

FIGURE 5. Initial mesh on box with two cylinders.

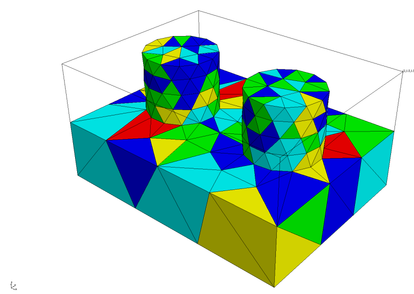

FIGURE 6. One level of partitioning of unstructured mesh.

# elements	ℓ	$\boldsymbol{H}$(curl)		$\boldsymbol{H}$(div)		Laplace	
		arithm.	oper.	arithm.	oper.	arithm.	oper.
242688	5	1.15	1.14	1.14	1.14	1.16	1.15
30336	4	1.15	1.15	1.14	1.14	1.18	1.17
3792	3	1.17	1.20	1.14	1.15	1.24	1.26
474	2	1.19	1.54	1.08	1.20	1.44	1.84

TABLE 6.2. Arithmetic and operator complexities for problems on the unit cube with unstructured mesh.

problems that are assembled from the preceding (finer) level element matrices. The same coarse information (coarse element matrices) is created also in $\mathcal{O}(N_k)$ operations. Thus the total setup cost is $\sum_{k=0}^{\ell} \mathcal{O}(N_k)$. The latter sum is $\mathcal{O}(N)$ (here $N = N_0$ is the finest

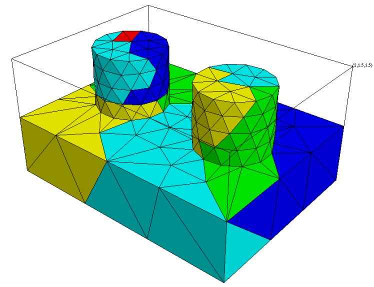

FIGURE 7. Two levels of partitioning of unstructured mesh.

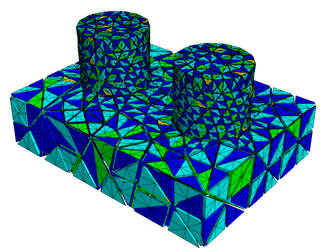

FIGURE 8. Partitioned refined mesh.

ℓ	$\boldsymbol{H}$(curl)			$\boldsymbol{H}$(div)			Laplace		
	N	MG	GS	N	MG	GS	N	MG	GS
5	430892	13	> 1999	720192	21	> 1999	65005	11	48
4	56094	11	> 1999	91472	18	> 1999	8911	9	23
3	7585	12	844	11796	15	> 1999	1326	8	11
2	1099	8	215	1565	15	614	227	5	4

TABLE 6.3. Number of iterations for problems on the box–cylinder with unstructured mesh; $\delta = 10^{-3}$.

level number of dofs) for any reasonable agglomeration strategy that we can control via the mesh partitioner used. The element agglomeration and the construction of the

# elements	ℓ	$\boldsymbol{H}$(curl)		$\boldsymbol{H}$(div)		Laplace	
		arithm.	oper.	arithm.	oper.	arithm.	oper.
354304	5	1.15	1.14	1.14	1.14	1.16	1.15
44288	4	1.15	1.15	1.14	1.14	1.18	1.16
5536	3	1.15	1.15	1.14	1.13	1.20	1.18
692	2	1.06	1.14	1.02	1.05	1.17	1.33

Table 6.4. Arithmetic and operator complexities for problems on the box–cylinder with unstructured mesh.

ℓ	# elements	# dofs (edges)	MG	GS	oper.	arithm.
2	692	1099	13	158	1.14	1.06
3	5536	7585	13	401	1.14	1.15
4	44288	56094	14	1092	1.15	1.15
5	354304	430892	17	>1999	1.14	1.15

Table 6.5. Numerical results for the $\boldsymbol{H}$(curl) problem on the box with two cylinders; $\delta = 1$.

ℓ	# elements	# dofs (edges)	MG	GS	oper.	arithm.
2	692	1099	8	215	1.14	1.06
3	5536	7585	11	844	1.15	1.15
4	44288	56094	11	>1999	1.15	1.15
5	354304	430892	13	>1999	1.14	1.15

Table 6.6. Numerical results for the $\boldsymbol{H}$(curl) problem on the box with two cylinders; $\delta = 10^{-3}$.

topology of the elements is typically much faster than the solution of the local finite element problems.

7. Conclusions

We have proposed new element agglomeration spaces that provide sequences of exact de Rham complexes. Although the existing AMGe convergence theory is limited to two levels, the new spaces when used to develop a $V(1,1)$–cycle algebraic preconditioner exhibit convergence close to that of the corresponding geometric multigrid algorithm on a structured grid.

Non–standard situations may occur if straightforward graph/mesh partitioners (like **metis**) are used to generate the agglomerated elements. Nevertheless, the sequence that does not use "edge" degrees of freedom, i.e., the pair Raviart–Thomas space $\mathbf{R}_H$ – piecewise constant space M_H, can be successfully coarsened without difficulty.

Extensions to higher order elements are feasible although perhaps not necessary for AMGe as higher order elements can be dealt with by a two-level algorithm involving smoothing and a preconditioner for the lower order case. The higher order element case would be potentially useful in up-scaling of linear and nonlinear PDEs.

References

[1] D. N. Arnold, R. S. Falk, and R. Winther, *Multigrid in $H(div)$ and $H(curl)$*, Numerische Mathematik **85**(2000), pp. 197–217.

[2] D. N. Arnold, R. S. Falk, and R. Winther, *Preconditioning in $H(div)$ and applications,* Mathematics of Computations **66**(1997), pp. 957–984.

[3] D. N. Arnold, R. S. Falk and R. Winther, *Differential complexes and stability of finite element methods I: The de Rham complex* in: "Compatible Spatial Discretizations" vol. 142 of the IMA Volumes in Mathematics and its Applications, Springer, Berlin, pp. 23-46.

[4] P. Bochev, C. Garasi, J. Hu, A. Robinson and R. Tuminaro, *An improved algebraic multigrid method for solving Maxwell's equations*, SIAM J. Sci. Comp. **25** (2003), 623–642.

[5] M. Brezina, A. J. Cleary, R. D. Falgout, V. E. Henson, J. E. Jones, T. A. Manteuffel, S. F. McCormick, and J. W. Ruge, *Algebraic multigrid based on element interpolation (AMGe)*, SIAM Journal on Scientific Computing, **22**(2000), pp. 1570-1592.

[6] F. Brezzi and M. Fortin, *Mixed and Hybrid Finite Element Methods*, Springer-Verlag, New York, 1991.

[7] T. Chartier, R. Falgout, V. E. Henson, J. Jones, T. Manteuffel, S. McCormick, J. Ruge, and P. S. Vassilevski, *Spectral element agglomerate AMGe,* in: Domain Decomposition Methods in Science and Engineering XVI, Lecture Notes in Computational Science and Engineering, Springer-Verlag, Berlin-Heidelberg, **55**(2007), pp. 515–524.

[8] R. Hiptmair, Multigrid method for H(div) in three dimensions, *Electronic Transaction on Numerical Analysis*, 6:133–152, 1997.

[9] R. Hiptmair, Multigrid method for Maxwell's equations. *SIAM Journal on Numerical Analysis*, 36(1):204–225, 1999.

[10] R. Hiptmair and A. Toselli, Overlapping and multilevel Schwarz methods for vector valued elliptic problems in three dimensions, in Parallel Solution of Partial Differential Equations, P. Bjorstad and M. Luskin, Eds., vol. 120 of IMA Volumes in Mathematics and its Applications, Springer, Berlin, 1999, pp. 181–202.

[11] R. Hiptmair, Finite elements in computational electromagnetism, *Acta Numerica*, **11**(2002), pp. 237–339.

[12] J. E. Jones and P. S. Vassilevski, AMGe based on element agglomerations, *SIAM Journal on Scientific Computing,* **23**(2001), pp. 109-133.

[13] G. Karypis and V. Kumar, A fast and high quality multilevel scheme for partitioning irregular graphs, *SIAM Journal on Scientific Computing*, **20**(1998), pp 359–392.

[14] T. V. Kolev and P. S. Vassilevski, *AMG by element agglomeration and constrained energy minimization interpolation,* Numerical Linear Algebra with Applications **13**(2006), pp. 771–788.

[15] F. Musy, L. Nicolas, and R. Perrussel, *Compatible coarse nodal and edge elements through energy functionals*, *SIAM Journal on Scientific Computing*, **29**(3)(2007), pp 1315–1337.

[16] S. Reitzinger and J. Schöberl, *An algebraic multigrid method for finite element discretization with edge elements*, Numerical Linear Algebra with Applications **9** (2002), 215–235.

[17] P. S. Vassilevski, Sparse matrix element topology with application to AMG and preconditioning, *Numerical Linear Algebra with Applications*, **9**(2002), pp. 429-444.

[18] P. S. Vassilevski and L. T. Zikatanov, *Multiple vector preserving interpolation mappings in algebraic multigrid,* SIAM J. Matrix Analysis and Applications **27**(2005–2006), pp. 1040–1055.

Department of Mathematics, Texas A&M University, College Station, TX 77843-3368, U.S.A.
E-mail address: pasciak@math.tamu.edu

Center for Applied Scientific Computing, Lawrence Livermore National Laboratory, P.O. Box 808, L-560, Livermore, CA 94551, U.S.A.
E-mail address: panayot@llnl.gov